Nanoprecipitated catestatin released from pharmacologically active microcarriers (PAMs) exerts pro-survival effects on MSC

Nanoprecipitated Catestatin released from pharmacologically active microcarriers (PAMs) exerts pro-survival effects on MSC

Angotti C[1], Venier-Julienne MC[2,3], Penna C[1], Femminò S[1], Sindji L[2,3], Paniagua C[4], Montero-Menei CN[2,3], Pagliaro P[1]**

*Equal contribution

1 Department of Clinical and Biological Sciences, University of Turin, Torino, Italy.

2 INSERM U 1066, Micro et Nanomédecines biomimétiques - MINT, Angers, France.

3 Université Angers, UMR-S1066 Angers, France.

4 Artificial Biopolymers Department, Institut des Biomolecules Max Mousseron (IBMM) UMR5247, CNRS, University of Montpellier, ENSCM, Montpellier, France.

Address for correspondence:

Prof Pasquale Pagliaro, M.D., Ph.D., O.M.P.S.
Associate Professor of Physiology
President of Italian Society of Cardiovascular Researches
http://www.sirc-cardio.it
Dpt Clinical and Biological Sciences
University of Torino, Italy
Tel. +390116705450
phax +390119038639
email: pasquale.pagliaro@unito.it

Abstract

Catestatin (CST), a fragment of Chromogranin-A, exerts angiogenic, arteriogenic, vasculogenic and cardioprotective effects. CST is a very promising agent for revascularization purposes, in "NO-OPTION" patients. However, peptides have a very short half-life after administration and must be conveniently protected. Fibronectin-coated pharmacologically active microcarriers (FN-PAM), are biodegradable and biocompatible polymeric microspheres that can convey mesenchymal stem cell (MSCs) and therapeutic proteins delivered in a prolonged manner. In this study, we first evaluated whether a small peptide such as CST could be nanoprecipitated and incorporated within FN-PAMs. Subsequently, whether CST may be released in a prolonged manner by functionalized FN-PAMs (FN-PAM-CST). Finally, we assessed the effect of CST released by FN-PAM-CST on the survival of MSCs under stress conditions of hypoxia-reoxygenation. An experimental design, modifying three key parameters (ionic strength, mixing and centrifugation time) of protein nanoprecipitation, was used to define the optimum condition for CST. An optimal nanoprecipitation yield of 76% was obtained allowing encapsulation of solid CST within FN-PAM-CST, which released CST in a prolonged manner. *In vitro,* MSCs adhered to FN-PAMs, and the controlled release of CST from FN-PAM-CST greatly limited hypoxic MSC-death and enhanced MSC-survival in post-hypoxic environment. These results suggest that FN-PAM-CST are promising tools for cell-therapy.

Key words: microcarriers, drug delivery, catestatin, mesenchymal stem cells, hypoxia

1. Introduction

Prolonged hypoxia an oxidative stress conditions are responsible of the damage observed in the cardiovascular system in several pathological situations; consequently prolonged effects of pro-survival factors are necessary tools to limit such a damage. Among emerging peptides in the cardiovascular system Chromogranin-A (CgA) derived peptides are occupying a role of paramount importance. CgA is a key player in the neuroendocrine regulation of cardiac function. In fact, CgA is ubiquitously distributed in the nervous system, immune system and diffuse neuroendocrine system of both vertebrates and invertebrates (Helle, 2004; Penna et al., 2012; Pieroni et al., 2007). CgA is a pro-hormone which is stored in vesicles (Taupenot et al., 2003) and its processing gives rise to several peptides of biological importance, including serpinin, pancreastatin, vasostatin, and Catestatin (CST) (Penna et al., 2012).

CST is a 21-amino acid derivate of CgA and initially it was described as a potent inhibitor of catecholamine release from adrenal medulla (Ratti et al., 2000; Tota et al., 2003), but in the last years several new biological activities have been described, including a cardioprotective role. Moreover a myocardial production of CST was demonstrated recently (Bassino et al., 2011; Bassino et al., 2015; Biswas et al., 2010; Penna et al., 2010; Penna et al., 2012; Perrelli et al., 2013). The anti-adrenergic effects of CST in the heart muscle seem to be mediated by the PI3K-Akt-eNO-Synthase signaling axis (Bassino et al., 2011; Bassino et al., 2015). Moreover a positive effect of CST on monocyte migration *in-vitro* and the induction of angiogenesis, arteriogenesis and vasculogenesis in the unilateral mouse hind limb ischemia model by a basic fibroblast growth factor (bFGF)-dependent mechanism has been demonstrated (Egger et al., 2008; Theurl et al., 2010). Based on the above-mentioned findings, it is clear that CST exerts a protective and proangiogenetic role *via* the activation of survival kinases.

Hence, CST is a very promising agent for cardiovascular protective purposes; however, usually, proteins have a very short half-life after administration and must be conveniently protected. The combination of cardioprotective agents and the use of biomaterials to improve cell behavior within the infarcted area is an interesting approach in cardiovascular regenerative medicine. Pharmacologically active microcarriers (PAMs), biodegradable and biocompatible polymeric microspheres containing a bioactive protein, have the ideal characteristics for this purpose. Besides being able to deliver physiological doses of a relevant bioactive protein released in a controlled manner, they may also convey cells on

their 3-dimensional (3D) biomimetic surface of extracellular matrix molecules. In this way the combined action of the bioactive protein and the biomimetic surface can favor the survival and engraftment of the transported cells after their transplantation in different pathological conditions (Delcroix et al., 2011; Karam et al., 2012; Musilli et al., 2012; Quittet et al., 2015; Savi et al., 2015; Tatard et al., 2007). Recently, it has been shown that PAMs releasing vascular-endothelial-growth-factor (VEGF) and conveying MSCs (derived from the adipose tissue) may induce their proliferation, angiogenic differentiation, and a decrease in cell death *in vitro* (Penna et al., 2013; Madonna et al., 2015). Moreover, in an *in vivo* mice model of post-ischemic myocardium these functionalized PAMs implanted in the infarcted myocardium enhanced MSC engraftment and differentiation into vascular structures resulting in myocardial fractional shortening improvement (Madonna et al., 2015). Within this line, obtaining a prolonged release of physiological doses of bioactive CST, a small peptide that can diffuse within the tissue parenchyma and exert cardioprotective properties, is an interesting strategy. The delivered peptide may not only repair the damaged tissue, but also in combination with the 3D biomimetic surface of the PAMs act synergistically to enhance the engraftment of the transported MSCs. Fibronectin-covered PAMs that stimulate MSC survival (Garbayo el at 2011) and CST, a catecholamine release inhibitor with antihypertensive, proangiogenetic and cardioprotective properties (Penna et al., 2012), may be a novel ideal combination to repair the organ damage caused by an hypoxic insult.

However, the prolonged and complete delivery of proteins at physiological doses still remains a technological challenge for effective clinical applications, mainly due to protein-polymer interaction during the process and protein degradation related to acidic environment following degradation of PLGA (D,L-lactide-co-glycolide acid) (Aubert-Pouessel et al., 2002; Park et al., 1998). With the aim to enhance protection of the protein from degradation and to obtain a more efficient release, we developed a strategy based on the use of a reversible nano-precipitated protein associated to a triblock copolymer P188 (poly (ethylene oxide) (PEO)- poly(propylene oxide) (PPO)-poly(ethylene oxide)PEO) leading to protein protection, especially during the release step (Giteau et al., 2008). Protein precipitates were formed from aqueous solution at the pH corresponding to the isoeletric point (pI) of the protein by the addition of sodium chloride to a water-miscible organic solvent, Glycofurol (Karam et al., 2014;).

Our purpose in this study is to determine an appropriate method of nanoprecipitation of this small peptide, CST, for the encapsulation in PLGA-based microspheres preserving CST bioactivity. P188 will be used as a component of the microcarrier covalently linked to PLGA (PLGA-P188-PLGA) to render it more hydrophilic, thus avoiding denaturation by adsorption to hydrophobic surfaces, but also to retain the protective polymer inside the microcarriers during their degradation (Morille et al., 2013). We thereafter evaluated the release kinetics of CST and the ability of the bioactive CST released from functionalized PAMs to protect bone marrow MSCs in standard *in vitro* conditions.

2. Materials and methods

2.1 Chemicals and drugs

Chemical reagents in general were purchased from Sigma Aldrich (St. Louis, MO, USA) unless otherwise stated. Polyvinyl alcohol (Mowiol® 4-88) was obtained from Kuraray Specialities Europe (Frankfurt, Germany). P188 poloxamer or Lutrol® was kindly supplied by BASF (Levallois-Perret, France). PLGA–P188–PLGA were synthesized by IBMM-CRBA CNRS UMR 5247 (Montpellier, France) as previoulsy described (Morille et al., 2013). Polytetrafluoroethylene (PTFE) filters Millex®-FH (pore size 0.45 μm) were obtained from Millipore (Millipore SA, Guyancourt, France). Culture mediums, penicillin, streptomycin and trypsin were obtained from M-Medical (Milan, Italy).

2.2 Protein precipitation and PAM formulation

Protein, glycofurol, and sodium chloride were used without further purification. Experiments were carried out at 4° C and the overall mixture was prepared directly inside a teflon tube. The protein powder was first dissolved in a non-buffered aqueous solution. In previous experiments (Karam et al., 2012, 2014), we showed that the best protein precipitation efficiency corresponds to the isoeletric point (pI) of the protein; for CST nanoprecipitation (pI CST 11.72). Then, we studied the possibility to adjust the pH of the solution by dissolving the salt into Glycine-NaOH buffer (pH 8.6). Sodium chloride was added at different concentrations, and at a later stage the poloxamer P188 was added in Glycine-Na-OH buffer to a 20:1 poloxamer-protein ratio; finally this solution was introduced into glycofurol. Thirty-minutes later at +4°C, the protein particles were recovered by centrifugation (10,000g, 30 min, +4°C). Mixing and centrifugation times were selected in order to optimize the quantity

of precipitated protein with an experimental design.

After this, microspheres where made by a non-denaturing solid-in-oil-in-water (s/o/w) emulsion evaporation/extraction technique (Delcroix et al., 2011). Protein precipitates were dispersed in the organic phase (670 µL of 50 mg PLGA or PLGA–P188–PLGA dissolved in a 3:1 methylene chloride:acetone solution). The organic suspension was then emulsified in a poly (vinyl alcohol) aqueous solution (30 mL, 4% w/v at 1 °C) and mechanically stirred at 550 rpm for 1 min. After addition of 33 mL of deionized water and stirring for 10 min, the emulsion was added to 167 mL deionized water and stirred for 20 min to extract the organic solvent. Finally, the microspheres were filtered on a 5 µm Small Volume Low Pressure (SVLP) type filter, washed and freeze-dried (Paillard-Giteau et al., 2010). PAM without protein were prepared following the same process, and called blank-microspheres (PAM) or FN-PAMs when covered with fibronectin (FN). To obtain FN-PAMs, PLGA-P188-PLGA microspheres were coated with FN and poly-D-Lysine (PDL). Coating solutions were prepared in Dulbecco's Phosphate-Buffered Saline DPBS.Each tube was covered with sigmacote® to prevent product loss on the tube walls. The concentration of the coating molecules was 9 µg/mL of FN and 6 µg/mL of PDL (corresponding to a 60:40 ratio of FN:PDL). 5 mg of PAM was added to DPBS and sonicated until full dispersion of the microspheres. The solution containing PDL and FN molecules was mixed to the microspheres suspension (final volume: 10 mL) and placed under rotation at 15 rpm at 37 °C during 1.5h. After coating, FN-PAMs were washed 3 times in distilled water, lyophilized and kept at − 20 °C.

2.3 PAM characterization

The surface morphology of the microspheres was investigated by scanning electron microscopy (SEM, JSM 6310F, JEOL, Paris, France). Freeze-dried microspheres were mounted onto metal stubs using double-sided adhesive tape, vacuum-coated with a film of carbon using a MED 020 (Bal-Tec, Balzers, Lichtenstein). The average particle size and size distribution were determined using a Coulter Multisizer (Beckman Coulter, Roissy, France). The microspheres were suspended in isotonic saline solution and sonicated for a few minutes prior to analysis. The mean particle sizes are expressed as volume distributions (N=3).

Zeta potential measurement was performed using a Zetasizer 2000 (Malvern Instruments,

Orsay, France) operating at 150 V at RT was used to assess the variations of electrical surface charges of PAMs. Briefly, a suspension of PAMs at 0.3 mg/ml in 1 mM NaCl was measured after sonication (42 kHz, 10 s). Results are presented after conversion of electrophoretic mobility values to zeta-potential using Smoluchowski's equation. Experiments were performed in triplicate (N=3).

The fibronectin surface was characterized by confocal microscopy after FN immunostaining. Lyophilized PAMs (1 mg) were suspended in DPBS containing 4% bovine serum albumin (BSA), 0.2% Tween 20 (DPBSBT) and incubated for 30 min at room temperature (RT) under 15 rpm stirring. Samples were then washed three times with DPBS and centrifuged (9000 g, 5 min, R.T.). Anti-FN mouse monoclonal antibody (1:100 in DPBSBT) was incubated at 37 °C for 1.5 h under rotation or overnight at +4°C. Samples were then washed 3 times before incubation with biotinylated anti-mouse IgG antibody (2.5 µg/mL in DPBS) for 1 h, at RT, under rotation. After three washes, samples were incubated with streptavidin–fluoroprobe 547 H (1:500 in DPBS) at RT, for 40 min, under rotation. Samples were observed under confocal microscopy (Olympus Fluoview^{TM} FV2 300, Rungis, France). Three independent experiments were performed and every condition was observed in triplicate.

2.4 Experimental design

To define the optimum conditions of protein precipitation, an experimental design was used. We performed a preliminary experimental design (2^{4-1} fractional factorial design) with the aim to study the effect of 4 parameters and 3 interactions between these factors, supposing to influence the CST precipitation yield: the centrifugation speed, the contact time of mixture and the ionic strength of the protein aqueous solution (NaCl or $ZnCl_2$ concentration). The studied interactions are: NaCl concentration- $ZnCl_2$ concentration, NaCl concentration-contact time, Time- $ZnCl_2$ concentration. The effect of the tested experimental factors was calculated using NEMROD software (Mathieu and Nony, 2000). Subsequently, the parameters identified as influent on protein precipitation yield, were optimised with a Doehlert matrix. This experimental design represents an optimal design for the spherical domain defined by the two factors and it allows a sequential approach (Giteau et al., 2008) . Experiments required for this design are described in Fig.1. It consists in a set of 7 distinct experiments uniformly distributed in a hexagonal plan (step 1). To approach the optimal conditions, three complementary experiments were added for the matrice expansion (step 2),

and two supplementary experiments were performed (step 3). The measured response was the precipitation efficiencies of CST (%). The same experiments were performed for each condition: this allowed a direct comparison of responses.

2.5 Protein encapsulation efficiency

Protein encapsulation yield was determined considering the CST total protein entrapped. Protein PLGA-P188-PLGA microspheres (5 mg) were dissolved in 500 µl Dimethylformamide (DMF) in Teflon™ tube and vortexed. After 10 min 500 µl of DMF was added and the solution was vortexed for 10 min more. The encapsulation efficiency was measured using NanoDrop 2000 Spectrophotometer (Thermo Scientific,France) immediately to avoid artifacts (N=3).

2.6 Release Kinetics

The release profile of protein from PLGA-P188-PLGA microspheres was determined by adding 500 µl of PBS buffer, pH 7.4 to 5 mg of PAM-CST into eppendorf tubes. The tubes were closed and incubated in a shaking water bath (37°C, 125 r.p.m.). The tubes were centrifuged for 5-min. at 2800 g and 500 µl of the supernatant were collected for analysis and replaced by fresh buffer. This procedure was repeated at different time-points (1, 2, 3, 4, 7, 10, 14 and 21 days) and the released CST present in the collected aliquots was measured by NanoOrange® protein quantification kit (Invitrogen, Cergy Pontoise, France) following the manufacturer's guidelines. The theoretical amount of CST present in the 5 mg PAM-CST was corrected using the results of the encapsulation yield, thus allowing the actual amount of CST contained in the PAM-CST to be established. The cumulative release of CST- A over time was then calculated. Three independent experiments were performed.

2.7 MSC isolation and cell culture

Mesenchymal stem cells were extracted from bone marrow of femurs of Wistar rats 6–12 months of age (weight 450–550 g; Janvier, Le Genest St Isle, France). MSCs were extracted by inserting a 21-gauge needle into the shaft of the bone and flushing with a solution of minimum essential medium eagle α (α-MEM) and 20% fetal bovine serum (FBS) (Sigma-Aldrich, Milan, Italy) implemented with 2 mM glutamine, 100 U/ml penicillin and 100 mg/ml streptomycin (Lonza); the cell suspension was filtered and cultured at 37°C. After 24-hrs the medium was replaced with α -MEM containing 10% FBS, 2 mM glutamine, 100 U/ml

penicillin and 100 mg/ml streptomycin. We allowed MSCs to grow up to passage 3 (P3), replacing the medium every 2–3 days as reported in the literature (Gallo et al., 2007; Muscari et al., 2005; Penna et al., 2008; Raimondo et al., 2006; Wang et al., 2003).

All animal experiments comply with the ARRIVE guidelines and are carried out in accordance with the U.K. Animals (Scientific Procedures) Act, 1986 and associated guidelines, EU Directive 2010/63/EU for animal experiments, as well as with the National Institutes of Health guide for the care and use of Laboratory animals (NIH Publications No. 8023, revised 1978). The animal protocols followed in this study were approved by the local "Animal Use and Care" committees (RR # 145674720268, dated 08/04/2013).

2.8 In vitro study: survival after hypoxia/reoxygenation with and without pre-treatment with free-CST, FN-PAMs or FN-PAM-CST

Experiments were carried out with MSCs alone or after pre-treatment of MSCs with either FN-PAMs, FN-PAM-CST or CST alone (free CST) in normoxic and hypoxic experimental condition, as previously described (Penna et al., 2013). Briefly, the bone marrow-MSCs were pre-treated with free CST (5 nM), FN-PAMs (0.5 mg) or FN-PAM-CST (0.5 mg) for 24-hrs. Before exposure to hypoxic condition, MSCs were incubated with trypsin-EDTA 0.25% solution and subjected to mild centrifugations (250–300 g for 5-min.) in order to separate cells from FN-PAMs or FN-PAM-CST. Then the medium was changed and cells were cultured in 2% FBS without treatment factors. Thereafter, subgroups of cells were subjected to a protocol of hypoxia/reoxygenation (H/R) (72/3 hrs) in a hypoxic chamber (INVIVO2 200, Belsar, Varese, Italy). Accordingly the groups considered in the study of cell survival were the following (Fig.2):

1) Untreated MSCs kept under standard conditions for 3-days (MSC- 3-N), and untreated MSCs exposed to H/R (MSC-3-H);

2) MSCs pre-treated with FN-PAM and kept under standard conditions (FN-PAM-3-N), and MSCs pre-treated with FN-PAMs and exposed to H/R (FN-PAM-3-H);

3) MSCs pre-treated with FN-PAM-CST and kept under standard conditions (FN-PAM-CST-3-N), and MSCs pre-treated with FN-PAM-CST and exposed to H/R (FN-PAM-CST-3-H);

4) MSCs pre-treated with free CST and kept under standard conditions (CST-3-N), and MSCs pre-treated with free CST and exposed to H/R (CST-3-H).

In other words and in brief, in each of the above four groups, we considered normoxic (-N) and hypoxic (-H) protocols for comparative purpose.

At the end of experiments, in triplicate in a blinded fashion, cell survival was assessed, using the cell viability test 3-(4,5-Dimethylthiazol-2-yl)-2,5-diphenyltetrazolium bromide (MTT) assay (Sigma-Aldrich, Italy) (Wang et al., 2003).

2.9 Statistical analysis

Data are presented as mean +/- SEM. Statistical significance was performed with t test or one-way ANOVA (post-hoc test Newman-Keuls Multiple Comparison Test) using GraphPad Prism. The results were considered significant when $P< 0.05$.

3. Results

3.1 Characterization of PAM

Morphological features of PAM and release profile of CST from PAM are reported in Fig 3-I and 3-II, respectively. The average diameter and size distribution of the resulting microspheres were evaluated using a Multisizer® Coulter Counter. We obtained microspheres with a diameter of 60 μm ± 22 (Fig. 3-Ia). The morphological aspect of MS, determined by scanning electron microscopy (SEM), showed a spherical shape (Fig. 3-Ib,c). To obtain FN-PAMs, PLGA-P188-PLGA microspheres were coated with FN and Poly-D-Lysine (PDL) (FN:PDL is 60:40). The microspheres had a zeta potential of 42,9±1,75 indicating the coating of PDL on their surface allowing cell attachment. The fibronectin surface characterized by confocal microscopy after FN immunostaining (Fig. 3-Id,e) showed that they were covered by this extracellular matrix protein.

3.2 Experimental design

N°Exp	NaCl	Contact time	Centrifugation speed	$ZnCl_2$	Nanoprecipitation yield
(nemrod)	M	Min	G	M	%
1	0	30	10 000	0	16.2
2	1	30	10 000	0.008	24.3
3	0	60	10 000	0.008	32.3

4	1	60	10 000	0	61.3
	1	60	10 000	0	63.4
5	0	30	16 000	0.008	15.5
6	1	30	16 000	0	27,4
7	0	60	16 000	0	32.5
8	1	60	16 000	0.008	34.0
	1	60	16 000	0.008	40.3

Table 1: Fractional factorial design and nanoprecipitation yields for each experiment.

The effects of the parameters studied and of the interactions between these parameters are shown in Table 1 and graphically represented in Fig. 4. Preliminary experiments, testing multiple parameters supposed influencing CST precipitation, reveal how centrifugation speed and use of $ZnCl_2$ have a negligible effect on nanoprecipitation yield of CST (Fig.4). As shown in Table 1, we obtain low percentage of nanoprecipitation yield using $ZnCl_2$ 0.008M in combination with different centrifugation speeds. However, the difference in the ionic strength of the protein aqueous solution, using NaCl instead of $ZnCl_2$, and the increased contact time of mixture have a positive effect (Fig.4) and lead to a higher nanoprecipitation yield (63.4%), as shown in Table 1. Subsequently, these two parameters identified as influent on protein precipitation yield, were optimised with a Doehlert matrix (Fig.5). We found that the optimal conditions to obtain a good percentage of CST nanoprecipitation of 76% of the initial protein (Step 3), was obtained by increasing the contact time of the mixture until 90 min. at a 2.175 M NaCl. Furthermore, in order to obtain a good precipitation yield the protein needs to be in a pH which is similar to its isoeletric point (Karam et al., 2014), so we dissolved the salt in Glycine-NaOH buffer (pH 8.6). This condition allowed to obtain the best protein precipitation efficiency.

3.3 Release of CST from FN-PAM-CST

The encapsulation yield of total protein into FN-PAM-CST was 62%. After the release kinetics study we found a continuous release of CST from these PAMs. The release profile showed a burst effect during the first 24 h of almost 50% of CST corresponding to 15 µg for 5mg of PAM (Fig.3-II). This initial burst is followed by a quite homogeneous and continuous release until the end of the release period. The total amount released in three weeks for 5 mg

PAMs corresponded to around 45 µg, which is within the range of the physiological doses of CST that may be used with around 1 mg PAMs *in vitro*. The release profile observed at the end of 3 weeks shows a cumulative release representing 100% of the entrapped protein.

3.4 Survival after H/R with and without pre-treatment with free CST, FN-PAMs or FN-PAM-CST

Data of survival analysis after H/R in pre-treated cells are presented as percent variation with respect to mean value of the cell count in control condition (MSC-3-N). To choose the optimal dose of CST, we performed experiments testing at least three different concentrations of free CST (5 nM, 10 nM and 2.5 µM). While the higher concentration resulted toxic (induced cell death), the two lower concentrations similarly increased cell survival (data no shown), thus we decided to continue to test the lower concentration and to use 0.5 mg PAMs/15x10^4 cells in order to obtain a similar concentration of CST in dishes in the following experiments. This proportion corresponds to what has been used in different experiments (Penna et al., 2010; Bassino et al., 2015).

As can be seen in Fig 6a, in the absence of pre-treatment (CTRL), the H/R protocol induced a 20% reduction in MSC number ($p< 0.01$ *vs* control). While this H/R protocol was unable to induce cell death in the presence of FN-PAM, in the presence of either free CST or FN-PAM-CST, the MSC continued to even proliferate despite the H/R protocol ($p< 0.01$ *vs* H/R only, for both). Therefore, pre-treatment with either CST and/or FN-PAM are able to counteract hypoxia effects.

We also analyzed MSC proliferative behavior in normoxia (Fig 6b) and found out that CST was able to induce a slight proliferation, which was ameliorated by FN-PAM-CST. In fact, in normoxia MSC proliferation increased significantly with FN-PAM-CST only.

These results suggest that there is no loss of bio-activity of CST after nanopreciptation procedure, which actually slightly improved the activity of free CST, when slowly released from FN-PAM. Moreover, in H/R experiments, pre-treatment with FN-PAM-CST not only limited cell mortality, but also improved cell growth.

4. Discussion

Catestatin is a promising agent for cardiovascular protective purposes and use of PAMs to convey MSCs, and/or to deliver CST could be a good approach to repair the damage observed in the cardiovascular system in several pathological situations. In this study, we

have hypothesized that a continuous release of physiological low doses of CST by FN-PAM may act on cells and counteract in a better way prolonged oxidative- and hypoxic-induced stress. Within this context, the major new findings of this study are: *1)* CST can be nano-precipitated in order to preserve its structure for encapsulation studies; 2) Nanoprecipitated CST can be encapsulated in FN-PAMs; 3) functionalized FN-PAMs can slowly release a bioactive CST; 4) FN-PAMs induce MSC proliferation in normoxia potentiated by the functionalization with CST and 5) FN-PAM-CST protect bone marrow MSC from hypoxia/reoxygenation stress.

The encapsulation and the sustained release of a protein from microspheres is a difficult task and depends on the physicochemical characteristics of each protein such as molecular weight, hydrophilicity and stability (Bilati et al., 2005). In particular, the low molecular weight of CST represented a challenge for the prolonged release of this small peptide in an active state from the microspheres. We have previously shown that proteins encapsulated under a nanosolid state within a PLGA polymer preserve their structure and integrity, allowing a better and prolonged release profile and the maintenance of their biological activity (Penna et al., 2013). In order to optimize the preparation of small peptides, various methods like spray-drying or spray-freeze drying have been reported (Lam et al., 2000; Wang et al., 2004). Even if these methods can generate protein particles, they have several disadvantages, such as the complexity of the technique, leading to low protein recovery and, above all, they may denature proteins. From an aqueous solution, protein precipitation can be induced for example with the addition of polymers or salts, with the reduction of the protein charge by changing the pH, or with the reduction of the dielectric constant by the addition of water-miscible organic solvents (Cleland and Jones, 1996) increasing ionic strength. The salt-induced precipitation is an extensively used method in biotechnology for separating target proteins from multi-components protein solutions as the first purification (Arakawa et al., 1991; Foster et al., 1971; Rothstein, 1994). In our experimental setup, a high amount of salt is necessary for CST nanoprecipitation and encapsulation, while preserving its bioactivity.

With the aim to determine an appropriate method of precipitation of CST for the encapsulation in PLGA-P188-PLGA microspheres preserving CST bioactivity we performed an experimental design testing different parameters. Indeed the ionic strength can be used to stimulate the salt induced precipitation: sodium chloride reduces the electrostatic repulsive interaction between the charged proteins, promoting in this way attractive hydrophobic

interaction (Tobler et al., 2000; Vonhippel and Wong, 1964). However the increase of ionic strength was limited by the solubility of the salt used (NaCl 2.175 M) and by the formation of artefacts during the mixing. Moreover, excess salt-induced precipitation may induce proteins to incorrectly fold or to form insoluble aggregates upon re-dissolution (Tobler et al., 2000). We have furthermore employed an organic solvent to induce the formation of fine protein particles. Nanosized protein particles were formed by the addition of excess glycofurol, an organic solvent miscible in water, to the aqueous solution (Giteau et al., 2008). Glycofurol has been previously used to induce the formation of nanosized solid protein particles (Giteau et al., 2008; Karam et al., 2014), but to our knowledge, this is the first time that such a small peptide (21-amino acids) is efficiently precipitated with this method. Another parameter tested in the experimental design was the time of incubation of the mix of CST with sodium chloride and organic solvents. We observed an increased percentage of nanoprecipitation yield correlated to the increase in time of incubation. We obtained in fact a very good CST precipitation at 90 minutes of incubation.

Furthermore, P188 poloxamer was added to the mix to co-precipitate with the protein. This non-ionic surfactant, comprised of hydrophobic and hydrophilic segments will surround and protect the protein by limiting its adsorption onto the hydrophobic surface of the PLGA polymer (Morille et al., 2013; Mustafi et al., 2008). It was co-precipitated with CST at the ratio of 1:20 of protein:additive polymer, and allowed a complete release of CST. This formulation allows a complete CST release from the PAMs, probably due to a better diffusion of the protein and an enhanced protection within the core. In this study CST precipitation with glycofurol, sodium chloride and P188 in optimum conditions allowed obtaining stabilization during the encapsulation process without loss of bioactivity. In particular, the hydrophilic P188, limiting the protein interaction with the PLGA hydrophobic polymer surface, protects the protein, increases their biological activity and may favor protein release into the media. Actually, PAMs containing higher proportions of free P188 with the same protein content enhance active protein release (Morille et al., 2013). Therefore, P188 may certainly influence active protein release from triblock PLGA-P188-PLGA PAMs. In fact, 50% of CST was released during the first 24h *in vitro.* Such an abundant release in the initial phase of a post-ischemic therapeutic approach may be a positive feature. Indeed the first phase of reperfusion is the more critical for tissue salvage (Penna et al., 2012). The later phases may be critical for tissue

repair and regeneration and a continuous slow release of a therapeutic peptide (e.g. VEGF and CST) released by microspheres transporting cells on their 3D functionalized surface may be beneficial for tissue engineering strategies (Elçin et al., 2001; Madonna et al., 2015). However, this needs to be ascertained *in vivo* for CST, and it should be ascertained whether other conditions, such as fibronectin coating, may affect the release of the active peptide.

As demonstrated by us and other authors, CST is a very promising agent for a cardiovascular protective purpose (Bassino et al., 2011; Bassino et al., 2015; Egger et al., 2008; Penna et al., 2010; Perrelli et al., 2013). In order to reduce damage observed in cardiovascular system following oxidative stress and prolonged hypoxic conditions, therapies with cell transplantation could represent a good strategy to follow; however approaches adapted to the varying conditions are needed. We have recently shown that VEGF-A as such or slowly released by FN-PAM can differently affect survival kinases and anti-apoptotic mediators, in stem cells (Penna et al., 2013).

On the basis of the above reported data, we have hypothesized that the prolonged release of CST by FN-PAM may act on cells and counteract in a better way prolonged hypoxic-induced stress. The *in vitro* study with CST-PAM suggested that it is possible to yield a good and effective complex to be used against hypoxia/reoxygenation damage. PAMs represents a multifunction vehicle that can be used in many contexts and with a variety of cells and proteins , and could be considered a new approach to improve MSC survival in the pathological hostile environment.

A way to improve the efficiency of cell graft, for instance, is to design a scaffold able to deliver a bioactive therapeutic protein that is released in a controlled manner but also a scaffold that provides a biomimetic surface. PAMs represent an efficient and adaptable device for tissue engineering; they are biodegradable and non-cytotoxic microcarriers that provide an adequate 3D support for cell culture and/or for their administration (Delcroix et al., 2010). Depending on the choice of the encapsulated protein and also of the molecule used for the biomimetic coating, PAM represents a multifunction vehicle that can be used in many contexts and with a variety of cells.

5. Conclusions

Our data are in line with the viewpoint that the use of FN-PAMs complexed with therapeutic proteins could be considered a new approach to improve cell survival in hostile environments such as inflammatory and post-ischemic tissue. Within this context, it has been previously shown that the 3D biomimetic support provided by FN-PAMs on their own, without delivering a therapeutic factor, already increases the survival of MSCs transported by these PAMs and implanted in the brain after global ischemia (Garbayo et al., 2011). Moreover, they enhanced the neuroprotective effect of the implanted MSCs.

In this *in vitro* study, we have shown that CST can be encapsulated into PAMs and that this functionalized PAMs can protect bone marrow MSC from hypoxia/reoxygenation injury. If confirmed in an appropriate pre-clinical model, this approach may be envisaged for future clinical studies on tissue regeneration.

Acknowledgements

We would like to thank Dr Fabien Violet and Dr Francesca Tullio for their invaluable support in performing some of the experiments. Also we thank the SCIAM "Service commun d'imagerie et d'analyse microscopique" for help with SEM and confocal images. We thank the Italo-French University (Galileo project) and RILO (MeccaSaric) of the University of Torino for financial support.

FIGURE CAPTATIONS

Fig.1: Spatial representation of experiments varying in the defined experimental domain for CST nanoprecipitation. The table represents the values of each studied factor (NaCl and Time) for the different experiments.

Fig.2: Protocols and time-lines for experimental groups in hypoxia/reoxygenation. Timing of various interventions is shown in relation to the onset of cell culture. Mesenchymal stem cells (MSCs) were kept at 21% O2 conditions for 1 day during the pre-treatments, subsequently they were subjected to 3 days hypoxia and 3 hrs reoxygenation. Fibronectin-coated pharmacologically-active-microcarriers (FN-PAM), FN-PAM incorporating CST (FN-PAM- CST) or free CST were added at time 0. For comparative purpose we considered normoxic (-N) and hypoxic (-H) protocols.

Fig.3: Panel I, PAM characterization. PAM size distribution had an average diameter of 60 μm (a). SEM images show a smooth surface and confirm the size distribution (b,c). The surrounding biomimetic coating was distributed homogenously at their surface as shown by the confocal image of fibronectin immunofluorescence (c, d). **Panel II, Cumulative release of CST from microspheres up to 21 days**. Each point represents the mean of triplicate experiments.

Fig.4: Parameters and interaction studied. Graphical representation of the effects of the parameters and interaction studied (Nemrod Software).

Fig.5: Graphical representation of the measured responses as precipitation efficiencies. In the 3D view of the experimental domain, the directions of variation of the factor values are represented by arrows and the results by dots.

*mean of three values :
(a) : 57±2%
(b) : 45 ±3.5%
(c) : 43±2%
(d) : 76±3.5%

Fig. 6: Panel a), Survival analysis. Cell growth in normoxia for 3-days (blue bar), and cell survival after 3-days hypoxia and 3-hrs reoxigenation (H/R) of MSC pretreatred or not with factors (free CST, FN-PAMs or FN-PAM-CST). Data are % variation with respect to mean value of MSCs kept under standard conditions for 3-days (MSC-3-N). Pre-treatment with FN-PAM-CST is able to counteract hypoxia-induceed cell number reduction.
Panel b), Proliferative analysis. Cell growth in normoxia for 3-days of MSC pretreatred or not with factors (free CST, FN-PAMs or FN-PAM-CST). Data are % variation with respect to mean value of MSCs kept under standard conditions for 3-days (MSC-3-N).
* P< 0,01 vs CTRL normoxia # P< 0,01 vs CTRL H/R

REFERENCES

Arakawa, T., Kita, Y., Carpenter, J.F., 1991. Protein--solvent interactions in pharmaceutical formulations. Pharm Res 8, 285-291.

Aubert-Pouessel, A., Bibby, D.C., Venier-Julienne, M.C., Hindre, F., Benoit, J.P., 2002. A novel in vitro delivery system for assessing the biological integrity of protein upon release from PLGA microspheres. Pharm Res 19, 1046-1051.

Bassino, E., Fornero, S., Gallo, M.P., Gallina, C., Femminò, S., Levi, R., Tota, B., Alloatti, G., 2015. Catestatin exerts direct protective effects on rat cardiomyocytes undergoing ischemia/reperfusion by stimulating PI3K-Akt-GSK3β pathway and preserving mitochondrial membrane potential. PLoS One 10:e0119790.

Bassino, E., Fornero, S., Gallo, M.P., Ramella, R., Mahata, S.K., Tota, B., Levi, R., Alloatti, G., 2011. A novel catestatin-induced antiadrenergic mechanism triggered by the endothelial PI3K-eNOS pathway in the myocardium. Cardiovasc Res 91, 617-624.

Bilati, U., Allemann, E., Doelker, E., 2005. Strategic approaches for overcoming peptide and protein instability within biodegradable nano- and microparticles. Eur J Pharm Biopharm 59, 375-388.

Biswas, N., Curello, E., O'Connor, D.T., Mahata, S.K., 2010. Chromogranin/secretogranin proteins in murine heart: myocardial production of chromogranin A fragment catestatin (Chga(364-384)). Cell Tissue Res 342, 353-361.

Cleland, J.L., Jones, A.J., 1996. Stable formulations of recombinant human growth hormone and interferon-gamma for microencapsulation in biodegradable microspheres. Pharm Res 13, 1464-1475.

Delcroix, G.J., Garbayo, E., Sindji, L., Thomas, O., Vanpouille-Box, C., Schiller, P.C., Montero-Menei, C.N., 2011. The therapeutic potential of human multipotent mesenchymal stromal cells combined with pharmacologically active microcarriers transplanted in hemi-parkinsonian rats. Biomaterials 32, 1560-1573.

Delcroix, G.J., Schiller, P.C., Benoit, J.P., Montero-Menei, C.N., 2010. Adult cell therapy for brain neuronal damages and the role of tissue engineering. Biomaterials 31, 2105-2120.

Egger, M., Beer, A.G., Theurl, M., Schgoer, W., Hotter, B., Tatarczyk, T., Vasiljevic, D., Frauscher, S., Marksteiner, J., Patsch, J.R., Schratzberger, P., Djanani, A.M., Mahata, S.K., Kirchmair, R., 2008. Monocyte migration: a novel effect and signaling pathways of catestatin. Eur J Pharmacol 598, 104-111.

Elçin, Y.M., Dixit, V., Gitnick G., 2001. Extensive in vivo angiogenesis following controlled release of human vascular endothelial cell growth factor: implications for tissue engineering and wound healing. Artif Organs 25, 558-565.

Foster, P.R., Dunnill, P., Lilly, M.D., 1971. Salting-out of enzymes with ammonium sulphate. Biotechnol Bioeng 13, 713-718.

Gallo, M.P., Ramella, R., Alloatti, G., Penna, C., Pagliaro, P., Marcantoni, A., Bonafe, F., Losano, G., Levi, R., 2007. Limited plasticity of mesenchymal stem cells cocultured with adult cardiomyocytes. J Cell Biochem 100, 86-99.

Garbayo, E., Raval A.P., Curtis, K.M., Della-Morte, D., Gomez, L.A., D'Ippolito, G., Reiner, T., Perez-Stable, C., Howard, G.A., Perez-Pinzon, M.A., Montero-Menei, C.N., Schiller, P.C., 2011 Neuroprotective properties of marrow-isolated adult multilineage-inducible cells in rat

hippocampus following global cerebral ischemia are enhanced when complexed to biomimetic microcarriers. J Neurochem 119, 972-988.

Giteau, A., Venier-Julienne, M.C., Marchal, S., Courthaudon, J.L., Sergent, M., Montero-Menei, C., Verdier, J.M., Benoit, J.P., 2008. Reversible protein precipitation to ensure stability during encapsulation within PLGA microspheres. Eur J Pharm Biopharm 70, 127-136.

Helle, K.B., 2004. The granin family of uniquely acidic proteins of the diffuse neuroendocrine system: comparative and functional aspects. Biol Rev Camb Philos Soc 79, 769-794.

Karam, J.P., Muscari, C., Montero-Menei, C.N., 2012. Combining adult stem cells and polymeric devices for tissue engineering in infarcted myocardium. Biomaterials 33, 5683-5695.

Karam, J.P., Muscari, C., Sindji, L., Bastiat, G., Bonafe, F., Venier-Julienne, M.C., Montero-Menei, N.C., 2014. Pharmacologically active microcarriers associated with thermosensitive hydrogel as a growth factor releasing biomimetic 3D scaffold for cardiac tissue-engineering. J Control Release 192, 82-94.

Lam, X.M., Duenas, E.T., Daugherty, A.L., Levin, N., Cleland, J.L., 2000. Sustained release of recombinant human insulin-like growth factor-I for treatment of diabetes. J Control Release 67, 281-292.

Madonna, R., Petrov, L., Teberino, M.A., Manzoli, L., Karam, J.P., Renna, F.V., Ferdinandy, P., Montero-Menei, C.N., Yla-Herttuala, S., De Caterina, R., 2015. Transplantation of adipose tissue mesenchymal cells conjugated with VEGF-releasing microcarriers promotes repair in murine myocardial infarction. Cardiovasc Res 108, 39-49.

Mathieu, D., Nony, J., 2000. R.P.T.L., 2000. NEMROD®-W (New Efficient Methodology for Research using Optimal Design). LPRAI-Marseille, Fr.

Morille, M., Van-Thanh, T., Garric, X., Cayon, J., Coudane, J., Noel, D., Venier-Julienne, M.C., Montero-Menei, C.N., 2013. New PLGA-P188-PLGA matrix enhances TGF-beta3 release from pharmacologically active microcarriers and promotes chondrogenesis of mesenchymal stem cells. J Control Release 170, 99-110.

Muscari, C., Bonafe, F., Stanic, I., Flamigni, F., Stefanelli, C., Farruggia, G., Guarnieri, C., Caldarera, C.M., 2005. Polyamine depletion reduces TNFalpha/MG132-induced apoptosis in bone marrow stromal cells. Stem Cells 23, 983-991.

Musilli, C., Karam, J.P., Paccosi, S., Muscari, C., Mugelli, A., Montero-Menei, C.N., Parenti, A., 2012. Pharmacologically active microcarriers for endothelial progenitor cell support and survival. Eur J Pharm Biopharm 81, 609-616.

Mustafi, D., Smith, C.M., Makinen, M.W., Lee, R.C., 2008. Multi-block poloxamer surfactants suppress aggregation of denatured proteins. Biochim Biophys Acta 1780, 7-15.

Paillard-Giteau, A., Tran, V.T., Thomas, O., Garric, X., Coudane, J., Marchal, S., Chourpa, I., Benoit, J.P., Montero-Menei, C.N., Venier-Julienne, M.C., 2010. Effect of various additives and polymers on lysozyme release from PLGA microspheres prepared by an s/o/w emulsion technique. Eur J Pharm Biopharm 75, 128-136.

Park, T.G., Yong Lee, H., Sung Nam, Y., 1998. A new preparation method for protein loaded poly(D, L-lactic-co-glycolic acid) microspheres and protein release mechanism study. J Control Release 55, 181-191.

Penna, C., Alloatti, G., Gallo, M.P., Cerra, M.C., Levi, R., Tullio, F., Bassino, E., Dolgetta, S., Mahata, S.K., Tota, B., Pagliaro, P., 2010. Catestatin improves post-ischemic left ventricular function and decreases ischemia/reperfusion injury in heart. Cell Mol Neurobiol 30, 1171-1179.

Penna, C., Perrelli, M.G., Karam, J.P., Angotti, C., Muscari, C., Montero-Menei, C.N., Pagliaro, P., 2013. Pharmacologically active microcarriers influence VEGF-A effects on mesenchymal stem cell survival. J Cell Mol Med 17, 192-204.

Penna, C., Raimondo, S., Ronchi, G., Rastaldo, R., Mancardi, D., Cappello, S., Losano, G., Geuna, S., Pagliaro, P., 2008. Early homing of adult mesenchymal stem cells in normal and infarcted isolated beating hearts. J Cell Mol Med 12, 507-521.

Penna, C., Tullio, F., Perrelli, M.G., Mancardi, D., Pagliaro, P., 2012. Cardioprotection against ischemia/reperfusion injury and chromogranin A-derived peptides. Curr Med Chem 19, 4074-4085.

Perrelli, M.G., Tullio, F., Angotti, C., Cerra, M.C., Angelone, T., Tota, B., Alloatti, G., Penna, C., Pagliaro, P., 2013. Catestatin reduces myocardial ischaemia/reperfusion injury: involvement of PI3K/Akt, PKCs, mitochondrial KATP channels and ROS signalling. Pflugers Arch 465, 1031-1040.

Pieroni, M., Corti, A., Tota, B., Curnis, F., Angelone, T., Colombo, B., Cerra, M.C., Bellocci, F., Crea, F., Maseri, A., 2007. Myocardial production of chromogranin A in human heart: a new regulatory peptide of cardiac function. Eur Heart J 28, 1117-1127.

Quittet, M.S., Touzani, O., Sindji, L., Cayon, J., Fillesoye, F., Toutain, J., Divoux, D., Marteau, L., Lecocq, M., Roussel, S., Montero-Menei, C.N., Bernaudin, M., 2015. Effects of mesenchymal stem cell therapy, in association with pharmacologically active microcarriers releasing VEGF, in an ischaemic stroke model in the rat. Acta Biomater 15, 77-88.

Raimondo, S., Penna, C., Pagliaro, P., Geuna, S., 2006. Morphological characterization of GFP stably transfected adult mesenchymal bone marrow stem cells. J Anat 208, 3-12.

Ratti, S., Curnis, F., Longhi, R., Colombo, B., Gasparri, A., Magni, F., Manera, E., Metz-Boutigue, M.H., Corti, A., 2000. Structure-activity relationships of chromogranin A in cell adhesion. Identification of an adhesion site for fibroblasts and smooth muscle cells. J Biol Chem 275, 29257-29263.

Rothstein, F., 1994. Differential precipitation of proteins. Science and technology. Bioprocess Technol 18, 115-208.

Savi, M., Bocchi, L., Fiumana, E., Karam, J.P., Frati, C., Bonafe, F., Cavalli, S., Morselli, P.G., Guarnieri, C., Caldarera, C.M., Muscari, C., Montero-Menei, C.N., Stilli, D., Quaini, F., Musso, E., 2015. Enhanced engraftment and repairing ability of human adipose-derived stem cells, conveyed by pharmacologically active microcarriers continuously releasing HGF and IGF-1, in healing myocardial infarction in rats. J Biomed Mater Res A 103, 3012-3025.

Tatard, V.M., Sindji, L., Branton, J.G., Aubert-Pouessel, A., Colleau, J., Benoit, J.P., Montero-Menei, C.N., 2007. Pharmacologically active microcarriers releasing glial cell line -

derived neurotrophic factor: Survival and differentiation of embryonic dopaminergic neurons after grafting in hemiparkinsonian rats. Biomaterials 28, 1978-1988.

Taupenot, L., Harper, K.L., O'Connor, D.T., 2003. The chromogranin-secretogranin family. N Engl J Med 348, 1134-1149.

Theurl, M., Schgoer, W., Albrecht, K., Jeschke, J., Egger, M., Beer, A.G., Vasiljevic, D., Rong, S., Wolf, A.M., Bahlmann, F.H., Patsch, J.R., Wolf, D., Schratzberger, P., Mahata, S.K., Kirchmair, R., 2010. The neuropeptide catestatin acts as a novel angiogenic cytokine via a basic fibroblast growth factor-dependent mechanism. Circ Res 107, 1326-1335.

Tobler, S.A., Sherman, N.E., Fernandez, E.J., 2000. Tracking lysozyme unfolding during salt-induced precipitation with hydrogen exchange and mass spectrometry. Biotechnol Bioeng 71, 194-207.

Tota, B., Mazza, R., Angelone, T., Nullans, G., Metz-Boutigue, M.H., Aunis, D., Helle, K.B., 2003. Peptides from the N-terminal domain of chromogranin A (vasostatins) exert negative inotropic effects in the isolated frog heart. Regul Pept 114, 123-130.

Vonhippel, P.H., Wong, K.Y., 1964. Neutral Salts: The Generality of Their Effects on the Stability of Macromolecular Conformations. Science 145, 577-580.

Wang, J., Chua, K.M., Wang, C.H., 2004. Stabilization and encapsulation of human immunoglobulin G into biodegradable microspheres. J Colloid Interface Sci 271, 92-101.

Wang, X., Willenbring, H., Akkari, Y., Torimaru, Y., Foster, M., Al-Dhalimy, M., Lagasse, E., Finegold, M., Olson, S., Grompe, M., 2003. Cell fusion is the principal source of bone-marrow-derived hepatocytes. Nature 422, 897-901.

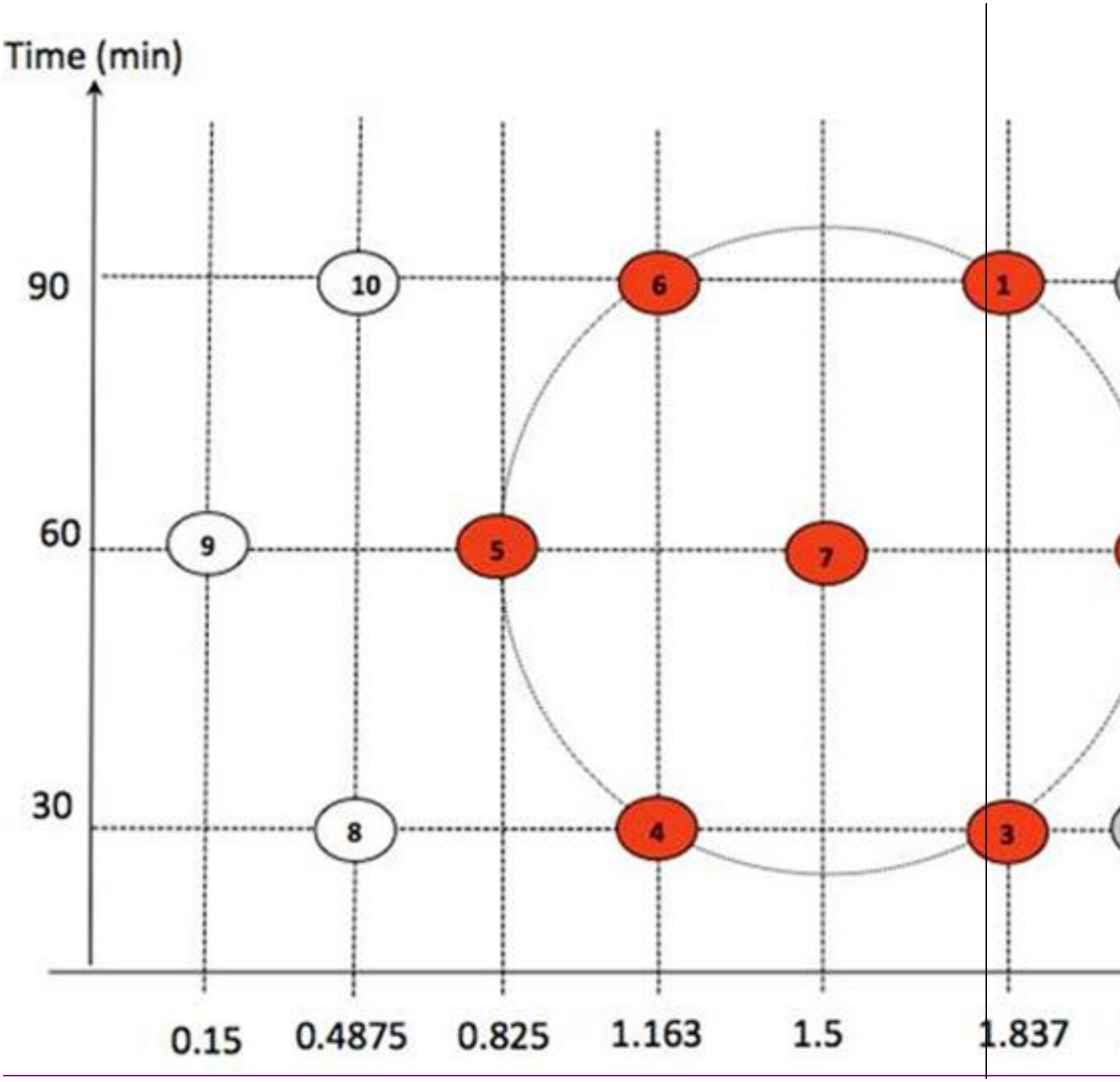
Time (min)
90
60
30
10
6
1
9
5
7
8
4
3
0.15
0.4875
0.825
1.163
1.5
1.837

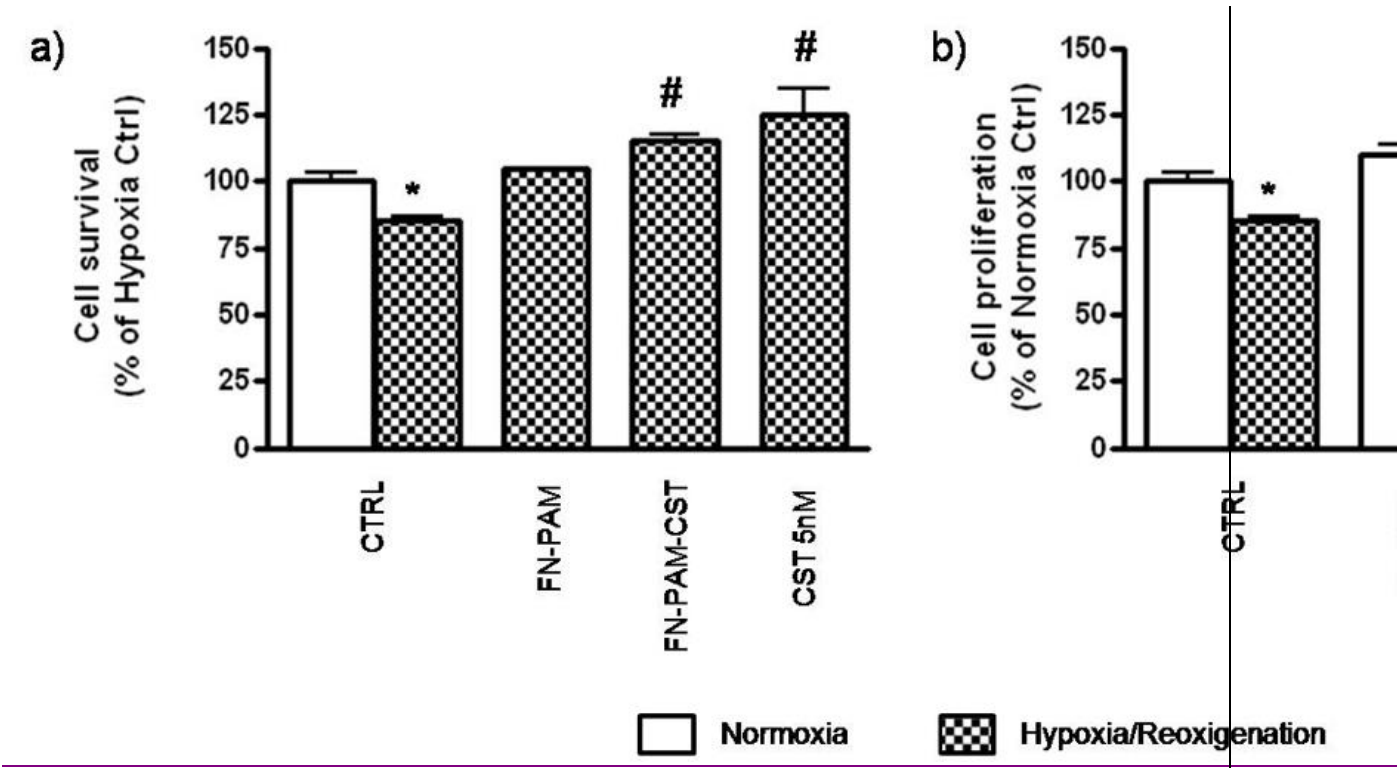
a)
Cell survival
(% of Hypoxia Ctrl)
150
125
100
75
50
25
0
*
#
#
CTRL
FN-PAM
FN-PAM-CST
CST 5nM
b)
Cell proliferation
(% of Normoxia Ctrl)
150
125
100
75
50
25
0
*
CTRL
Normoxia
Hypoxia/Reoxigenation

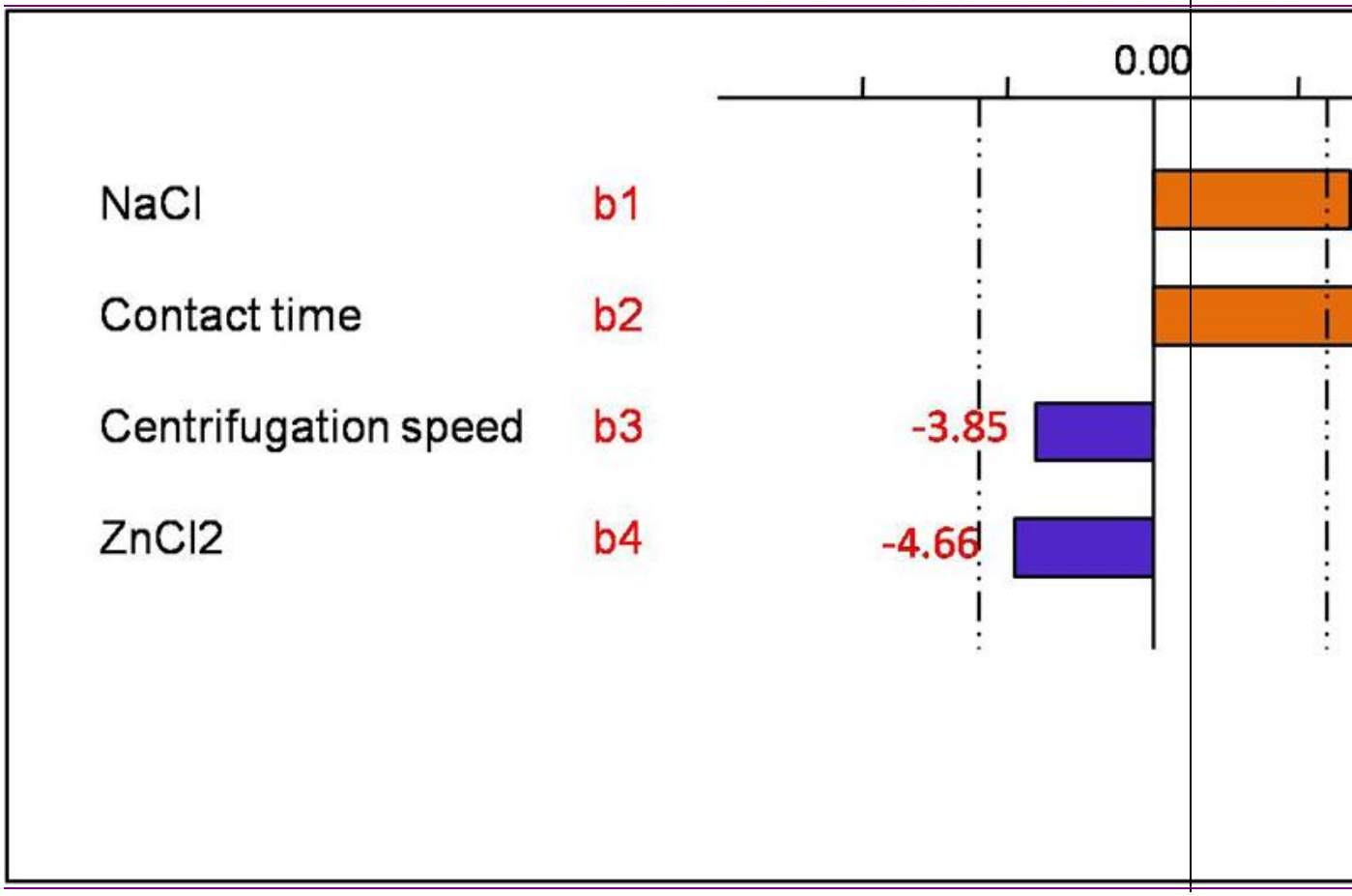
0.00
NaCl
b1
Contact time
b2
Centrifugation speed
b3
-3.85
ZnCl2
b4
-4.66

I)

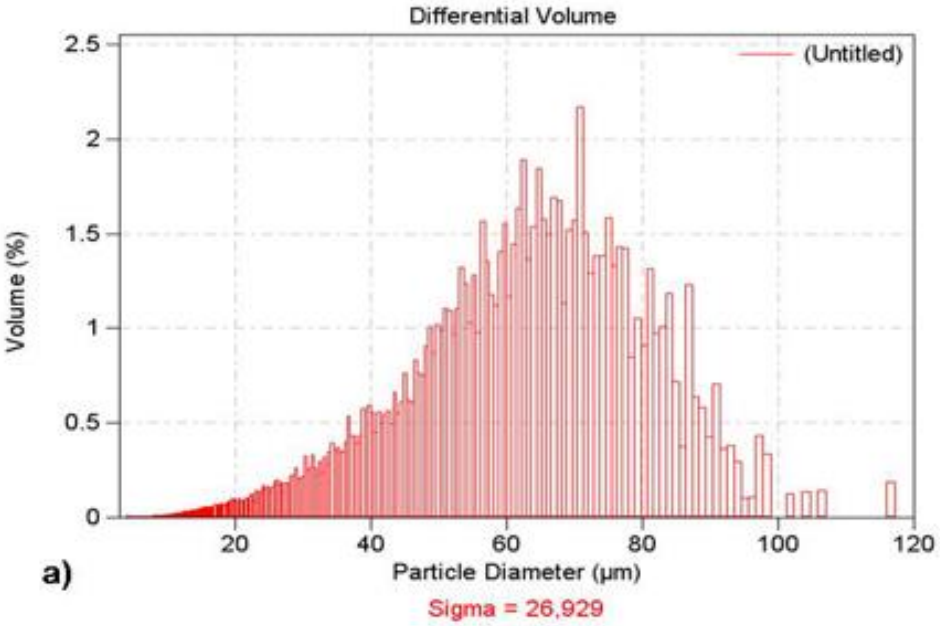
Differential Volume
(Untitled)
Volume (%)
2.5
2
1.5
1
0.5
0
20
40
60
80
100
120
Particle Diameter (µm)
Sigma = 26,929

a)

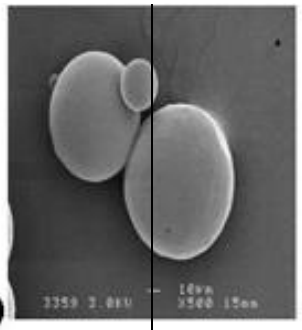

b)

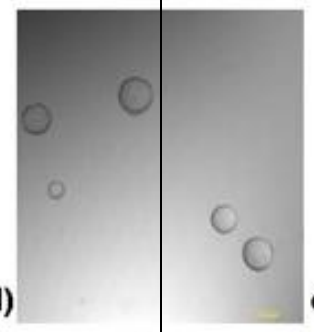

d)

II)

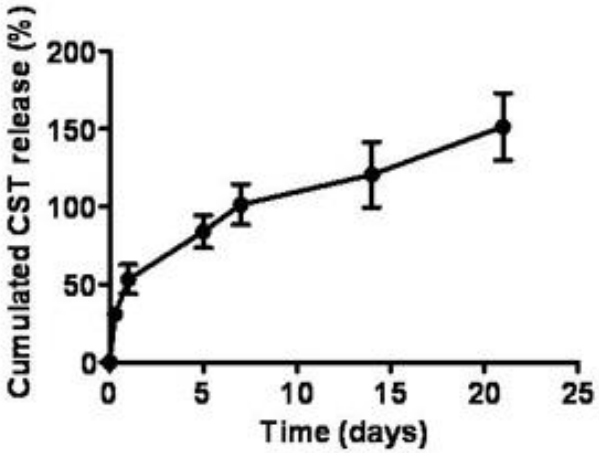
Cumulated CST release (%)
200
150
100
50
0
0
5
10
15
20
25
Time (days)

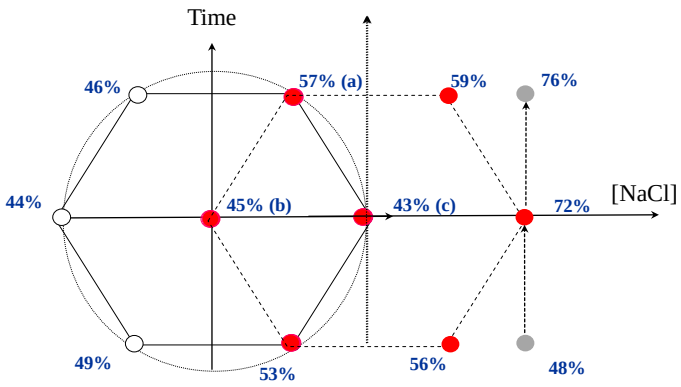
Time
46%
57% (a)
59%
76%
44%
45% (b)
43% (c)
72%
[NaCl]
49%
53%
56%
48%

680

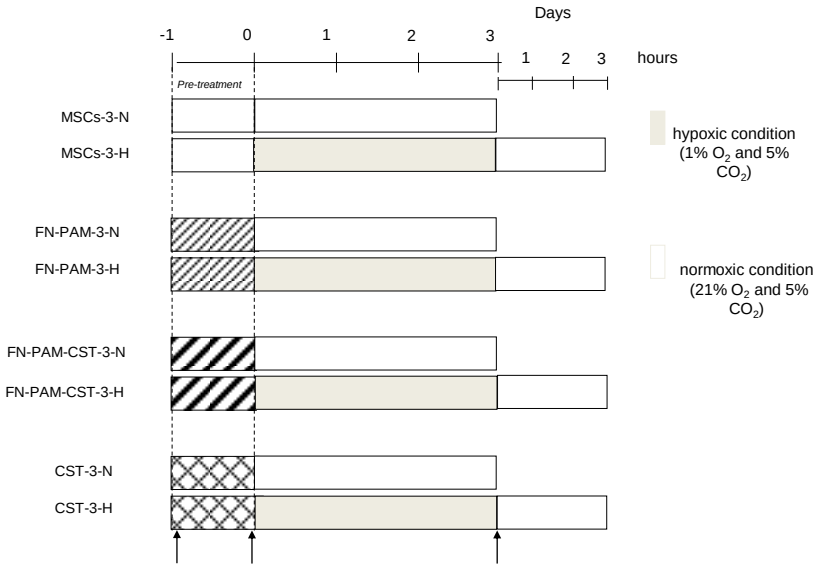
Days
-1
0
1
2
3
1
2
3
hours
Pre-treatment
MSCs-3-N
MSCs-3-H
FN-PAM-3-N
FN-PAM-3-H
FN-PAM-CST-3-N
FN-PAM-CST-3-H
CST-3-N
CST-3-H
hypoxic condition (1% O2 and 5% CO2)
normoxic condition (21% O2 and 5% CO2)